Journal of
PERIODONTAL RESEARCH

J Periodont Res 2016

JOURNAL OF PERIODONTAL RESEARCH
doi:10.1111/jre.12345

The silencing of cathepsin K used in gene therapy for periodontal disease reveals the role of cathepsin K in chronic infection and inflammation

W. Chen[1,*], B. Gao[1,2,*], L. Hao[1,2], G. Zhu[1], J. Jules[1], M. J. MacDougall[3], J. Wang[1], X. Han[4], X. Zhou[2], Y.-P. Li[1]

[1]Department of Pathology, University of Alabama at Birmingham, Birmingham, AL, USA, [2]The State Key Laboratory of Oral Diseases, West China College of Stomatology, Sichuan University, Chengdu, Sichuan, China, [3]Institute of Oral Health Research, School of Dentistry, University of Alabama at Birmingham, Birmingham, AL, USA and [4]Department of Immunology and Infectious Disease, The Forsyth Institute, Cambridge, MA, USA

Chen W, Gao B, Hao L, Zhu G, Jules J, MacDougall MJ, Wang J, Han X, Zhou X, Li Y-P. The silencing of cathepsin K used in gene therapy for periodontal disease reveals the role of cathepsin K in chronic infection and inflammation. J Periodont Res 2016; doi:10.1111/jre.12345. © 2016 John Wiley & Sons A/S. Published by John Wiley & Sons Ltd

Background and Objective: Periodontitis is a severe chronic inflammatory disease and one of the most prevalent non-communicable chronic diseases that affects the majority of the world's adult population. While great efforts have been devoted toward understanding the pathogenesis of periodontitis, there remains a pressing need for developing potent therapeutic strategies for targeting this dreadful disease. In this study, we utilized adeno-associated virus (AAV) expressing cathepsin K (Ctsk) small hairpin (sh)RNA (AAV-sh-Ctsk) to silence Ctsk *in vivo* and subsequently evaluated its impact in periodontitis as a potential therapeutic strategy for this disease.

Material and Methods: We used a known mouse model of periodontitis, in which wild-type BALB/cJ mice were infected with *Porphyromonas gingivalis* W50 in the maxillary and mandibular periodontium to induce the disease. AAV-sh-Ctsk was then administrated locally into the periodontal tissues *in vivo*, followed by analyses to assess progression of the disease.

Results: AAV-mediated Ctsk silencing drastically protected mice (> 80%) from *P. gingivalis*-induced bone resorption by osteoclasts. In addition, AAV-sh-Ctsk administration drastically reduced inflammation by impacting the expression of many inflammatory cytokines as well as T-cell and dendritic cell numbers in periodontal lesions.

Conclusion: AAV-mediated Ctsk silencing can simultaneously target both the inflammation and bone resorption associated with periodontitis through its inhibitory effect on immune cells and osteoclast function. Thereby, AAV-sh-Ctsk administration can efficiently protect against periodontal tissue damage and alveolar bone loss, establishing this AAV-mediated local silencing of Ctsk as an important therapeutic strategy for effectively treating periodontal disease.

Xuedong Zhou, PhD, The State Key Laboratory of Oral Diseases, West China College of Stomatology, Sichuan University, Chengdu, Sichuan 610041, China
Tel: 86-28-5501480
Fax: 86-28-5582167
e-mail: zhouxd@scu.edu.cn
Yi-Ping Li, PhD, Department of Pathology, University of Alabama at Birmingham, SHEL 810, 1825 University Blvd, Birmingham, AL 35294-2182, USA
Tel: +1205 975 2606
Fax: +1205 975 4919
e-mail: ypli@uab.edu
*These authors contributed equally to this work.

Key words: adeno-associated virus; alveolar bone loss; cathepsin K; gene therapy; periodontal diseases

Accepted for publication October 11, 2015

Periodontitis, affecting the oral health of most adult Americans, is a chronic inflammatory disease that damages the soft tissue and destroys the alveolar bone that supports the teeth, which ultimately lead to tooth loss. Whereas most studies indicate that periodontitis is caused by polymicrobial infection, there is evidence that the extent of the inflammation in periodontitis may also result from interaction between select species of the oral microflora and the host immune response (1–3). Nevertheless, *Porphyromonas gingivalis* W50 has been appointed as one of the most prominent pathogens highly associated with periodontitis (4,5). Notably, the inflammatory spectrum associated with the host response in gingival tissues triggers enhanced bone resorption by osteoclasts, the body's sole bone-resorbing polykaryons, for the resulted tooth loss. Osteoclasts originate from monocytic precursors of the hematopoietic lineage by stimulation with the receptor activator of the NF-κβ ligand (RANKL) and macrophage colony-stimulating factor (M-CSF). Moreover, numerous inflammatory cytokines, including tumor necrosis factor alpha α (TNFα), interleukin (IL)-1 and IL-6 can also promote osteoclast formation and/or function.

Cathepsin K (Ctsk) is a lysosomal cysteine protease that belongs to the peptidase C1 protein gene family (6). Ctsk is strongly expressed by osteoclasts and specifically induced during osteoclast differentiation through stimulation of osteoclast precursors with M-CSF and RANKL. As such, Ctsk is highly considered a good marker gene for osteoclasts. In particular, Ctsk functions by degrading the protein components of the bone matrix, which is critical for osteoclastic bone resorption. Hence, inactivating mutations, which affect Ctsk function, have resulted in pycnodysostosis in humans, a disease characterized by impaired bone resorption (7). Given its crucial role and specific expression in osteoclasts, Ctsk is often considered as an important therapeutic target for targeting bone loss in many bone diseases of excessive osteoclast formation and/or functions, including rheumatoid arthritis, postmenopausal osteoporosis and periodontal disease.

Adeno-associated virus (AAV) gene silencing is a new and potent strategy that has been utilized in many clinical studies to target many pathological disorders (8). Specifically, AAV therapy can insert specific genes with great certainty into the genome to maintain long-term and sustainable gene expression in diseases resulted from defective gene expression and/or function. Furthermore, novel strategies have been devised to employ AAV *in vivo* to induce long-term and potent silencing of specific genes associated with disease outcomes through local administration (9). Importantly, aside from the mild immune response elicited, numerous studies have demonstrated that AAV administration is not only safe but is also well tolerated by patients (10). Hence, given the essential role of Ctsk in osteoclast function and the favorable characteristics of AAV-mediated gene therapy, we hypothesized that targeting Ctsk inhibits the inflammation and bone loss caused by bacterial infection in periodontitis. To test our hypothesis, we employed AAV-mediated RNA interference to investigate the effects of Ctsk silencing in a mouse model of periodontitis. This study was aimed at examining conclusively the therapeutic potential of Ctsk depletion *in vivo* via local administration of AAV-sh-Ctsk to reduce tissue damage from inflammation and bone resorption in periodontitis induced by *P. gingivalis* W50.

Material and methods

Animals

Wild-type (WT) female BALB/cJ mice were obtained from the Jackson Laboratory for the study. The animals were housed in the University of Alabama at Birmingham (UAB) animal facility and were given food and water ad libitum. All experimental protocols were approved by the NIH and the UAB Institutional Animal Care and Use Committee. Animal protocol related to this study is (animal protocol number 131209236). Please refer to Data S1 – Table S1 for detailed information.

Design and construction of small hairpin RNA

To design a small hairpin RNA (shRNA) construct that can effectively knockdown Ctsk, we used the Dharmacon siDESIGN center (http://www.dharmacon.com) as described in our recent publication (11). The Ctsk shRNA oligonucleotide (5′-GATCCC C-GAGGTGTGTACTATGATGAA A-TTCAAGAGA-TTTCATCATAG TACACACCTCTTTTTGGAAT-3′) was annealed and cloned downstream of the H1 promoter in the AAV-H1 vector (gift from Dr. Sergei Musatov) into *Bgl*II and *Hin*dIII sites to generate the AAV-H1-shRNA-Ctsk construct. The AAV-H1-shRNA-luc construct (gift from Dr. Sergei Musatov) contains a luciferase gene and a yellow fluorescent protein (YFP) expression cassette and was used as a control vector for both the shRNA and AAV, as in previous studies (12). The BLAST homology search predicted that the control shRNAs would not affect Ctsk or any other known mouse gene (12).

Adeno-associated virus–small hairpin RNA viral production and purification

We utilized the AAV Helper-Free System (AAV Helper-Free System; Stratagene, San Diego, CA, USA) for viral production using a triple transfection, helper-free method, and purified as described in a previous study but with slight modification (13). Briefly, HEK 293 cells were transduced with pAAV-shRNA, pHelper and pAAV-RC plasmids (Stratagene) using the calcium phosphate method. Cells are collected after 60–72 h and lysed with chloroform at 37°C for 1 h. Sodium chloride was then added before shaking the cells at room temperature for 30 min. The stock was then spun at 10,000 *g* for 15 min and the supernatant was collected and cooled on ice for 1 h with PEG8000. The solution was spun at 9000 *g* for 15 min, and then the pellet was trea-

ted with DNase and RNase. After the addition of chloroform and centrifugation at 10,000 *g* for 5 min, the purified virus was in the aqueous phase at viral particle numbers of 1×10^{10}/mL. The AAV particle titer was determined by AAV Quantitation Titer Kit (Cell Biolabs, San Diego, CA, USA).

The viral vectors were evaluated for their ability to infect target tissue as previously described (14). Briefly, optimal viral particle numbers for infection were determined from the percentage of target cells expressing YFP. To confirm the effect of Ctsk silencing, we examined the expression of Ctsk in osteoclasts using western blot and immunofluorescence. Luciferase expression vector AAV2-Luc was purchased from the University of North Carolina (Chapel Hill, NC, USA). The AAV2-Luc was injected into the right side of the lower jaw one time and luciferase expression was measured by the IVIS Imaging System 100 Series (Xenogen Corporation, Alameda, CA, USA) after 2 or 5 wk.

In vitro bone resorption assays

Bone resorption pits were assessed as described in previous studies (15,16). Mouse bone marrow (MBM) cells seeded on bovine cortical bone slices plated in 24-well dishes were transduced with viral vectors after 72 h of RANKL and M-CSF. Bone slices were harvested after stimulation of infected MBM cells with M-CSF and RANKL for three additional d, and culture media were also collected. Cells were removed from the bone slices with 0.25 M ammonium hydroxide and mechanical agitation. Bone slices were subjected to scanning electron microscopy (SEM) using a Philips 515 SEM (Amsterdam, the Netherlands) (Department Materials Engineering, UAB). Bone resorption was also assessed using wheat germ agglutinin (WGA) to stain exposed bone matrix proteins. Assays were quantified by measuring the percentage of the areas resorbed in three randomly selected sites using the ImageJ analysis software (Wayne Rasband, NIH, Bethesda, MD, USA).

Cells and cell culture

Pre-osteoclasts and mature osteoclasts were generated from MBM as previously described (11,17). Briefly, MBM was obtained from tibiae and femora from 6 wk old female WT BALB/cJ mice. MBM cells 1×10^5 and 1×10^6 were seeded per well of 24- and six-well plates, respectively. MBM cells were cultured in α-modified Eagle's medium (Life Technologies, Grand Island, NY, USA) with 10% fetal bovine serum (Life Technologies) containing 10 ng/mL M-CSF (R&D Systems, Minneapolis, MN, USA) for 24 h. Subsequently, cells were cultured with 10 ng/mL RANKL (R&D Systems) and 10 ng/mL M-CSF for an additional 48 or 96 h to generate pre-osteoclasts or mature osteoclasts.

Western blotting analysis

Western blotting was performed as previously (17,18) and visualized and quantified using a Fluor-S Multi-Imager with Multi-Analyst software (Bio-Rad, Hercules, CA, USA). We utilized a rabbit anti-Ctsk antibody previously generated in our lab (11) and a goat antirabbit IgG-horseradish peroxidase (7074S; Cell Signaling, Danvers, MA, USA) for this western blot analysis.

Infection with *P. gingivalis* W50

P. gingivalis W50 (ATCC: 53978) was cultured on sheep's blood agar plates supplemented with hemin and vitamin K for 3 d. Single clones were harvested and transferred to trypticase soy broth supplemented with hemin and vitamin K. On day 4, bacteria were harvested, resuspended, and bacterial concentration was accessed at optical density readings 600 nm (1 optical density unit = 6.67×10^8 bacteria). Cell density was then adjusted to 10^{10} cells/mL in 0.2 mL of phosphate-buffered saline (PBS) containing 2% carboxymethylcellulose (Sigma-Aldrich, St. Louis, MO, USA) to prepare the infectious-bacterial solution. Periodontal infection was performed using 20 μL of infectious-bacterial solution as described in previous studies (15,16). In brief, all animals received antibiotic treatment for 3 d before infection, to reduce the original oral flora, followed by 3 d of an antibiotic-free period before submission to oral inoculation with a dental microbrush (Henry Schein, Duryea Road Melville, NY, USA) once per day for four consecutive d. To monitor bacterial colonization, murine oral cavities were sampled under sterile conditions on day 14 after infection for identification of *P. gingivalis* W50.

Adeno-associated virus–small hairpin–cathepsin K transduction of *P. gingivalis* W50-infected mice

We administrated AAV-sh-Ctsk in a site-specific manner as described in a previous study but with minor modifications (12). Briefly, mice were anesthetized via peritoneal injection with ketamine (62.5 mg/kg) and xylazine (12.5 mg/kg). Four d after the initial infection, mice were given either AAV-sh-Ctsk or AAV-sh-luc-YFP once per day for seven consecutive d. Specifically, mice were injected approximately 0.3–0.5 mm above the gingival margin of the maxillary molars on the right and left palatal aspects with 3 μL containing of either AAV-sh-Ctsk or AAV-sh-luc-YFP viral vector using a Hamilton syringe attached to a microinfusion pump (World Precision Instruments, Sarasota, FL, USA). As a negative control (normal), mice were not infected with *P. gingivalis* W50 or treated with viral vectors. As a positive control (disease), *P. gingivalis* W50-infected mice were not injected with viral vector. The detailed experimental strategy is provided in Fig. S1.

Harvest and preparation of tissue samples

Animals were killed by CO_2 inhalation 56 d after the first infection. The maxillae were removed and hemisected. Samples from the left side were defleshed in 2.6% sodium hypochlorite for bone measurement analysis as previously determined (15,16). Subse-

quently, maxillae samples from the right side were immediately fixed in 4% paraformaldehyde (PFA) and prepared for histological analysis according to standard protocol but with minor modifications. In brief, samples for paraffin sections were fixed in 4% PFA for 24 h, washed with PBS, decalcified in 10% of ethylenediaminetetraacetic acid in 0.1 M Tris solution (pH 7.0) for 10 d with daily replenishment, washed with PBS and embedded in paraffin after series dehydration. Low jaw samples from the right and left sides in independent experiment were collected for real-time quantitative polymerase chain reaction (qRT-PCR) analyses and enzyme-linked immunosorbent assays (ELISAs). Gingival tissues and/or alveolar bone were isolated under a surgical microscope. Gingival tissues and alveolar bone from right samples were pooled for qRT-PCR, and gingival tissues from right samples were pooled for ELISAs for cytokines.

Histological analysis

For paraffin sections, tissue were fixed by 4% PFA for 24 h, and then decalcified by 10% ethylenediaminetetraacetic acid for 10 d with daily replenishment before embedding in paraffin. For osteoclast analysis, tartrate-resistant acid phosphatase (TRAP) staining was performed and TRAP-positive osteoclasts were counted as described (16). Tissue sections were deparaffinized and hydrated through xylene and graded alcohol series, preincubated with 50 mM sodium acetate and 40 mM potassium sodium tartrate buffer for 20 min and then incubated with TRAP substrate solution for glycerol jelly. The histological analysis was carried out as previously described with slight modification (16), multinucleated TRAP-positive cells (> 3 nuclei) were counted in two different areas (i.e. the alveolar bone and periodontal ligament areas). The measurements consisted of measuring three different parts in the periodontal ligament area, i.e. coronal, middle and apical location. To ensure accurate analysis, we used series section (at least three sections) for width calculation.

Bone loss measurements

Analysis of bone loss was performed as previously described (15,16). Briefly, images of molar tooth roots and alveolar bone were captured using digital microscopy followed by analysis using Adobe PhotoshopTM (Adobe Systems, San Jose, CA, USA). The polygonal area enclosed by the cemento-enamel junction, the lateral margins of the exposed tooth root, and the alveolar ridge was measured using the ImageJ analysis software (Wayne Rasband, NIH). Measurements were expressed in mm^2.

Immunofluorescence staining

Immunofluorescent (IF) staining analysis was carried as indicated previously (19,20), except that anti-Ctsk rabbit polyclonal, anti-CD3 (Santa Cruz, Dallas, TX, USA) and Armenian hamster antimouse CD11c (Biolegend, San Diego, CA, USA) were used as primary antibody. Data were imaged using epifluorescence on a Zeiss Axioplan microscope (Ontario, CA, USA) in the Developmental Neurobiology Imaging and Tissue Processing Core at the UAB Intellectual and Disabilities Research Center. Nuclei were visualized with 4′,6-diamidino-2-phenylindole (Sigma-Aldrich, St. Louis, MO, USA).

Real-time quantitative polymerase chain reaction analysis

qRT-PCR analysis was performed as described (15,16) using TaqMan probes from Applied Biosystems (Foster City, CA, USA) according to the manufacturer's instructions. Briefly, cDNA was amplified by TaqMan® Fast Advanced Master Mix (Applied Biosystems, Life Technologies, Grand Island, NY, USA) (Table S2). Amplification reaction was carried via the Step-One *Plus* real-time PCR system (Applied Biosystems, Life Technologies). *Hprt* (hypoxanthine–guanine phosphoribosyl transferase) was used as endogenous control for gene expression analysis calculated as ratio of *Hprt* (deltaCT).

Enzyme-linked immunosorbent assay analysis

ELISA was performed in tissue extracts as previously described (15,16). These assays were carried out using commercial kits for IL-1α and IL-10 (BioLegend) and TNFα, IL-12, IL-6, interferon gamma and IL-17α (eBioscience, San Diego, CA, USA) according to the manufacturers' instructions. Data were reported as pg cytokine/mL.

Data quantification and statistical analyses

All experiments were repeated three times. Results were reported as mean ± SD. All experiments were performed in triplicate on three independent occasions. For the parametric data: bone loss measurements, histological analyses, qRT-PCR and ELISA data were analyzed with ANOVA and $p < 0.05$ was considered significant. For the non-parametric data: IF data were analyzed with the Mann–Whitney *U*-test, $U > 1.96$ was denoted as $p < 0.05$.

Results

Ctsk silencing by adeno-associated virus impairs osteoclastic bone resorption *in vitro*

To target bone resorption in periodontitis, we first used AAV-mediated gene therapy to silence Ctsk through an AAV-sh-Ctsk construct, which contains the YFP expression cassette *in vitro*. We used the AAV-sh-luc-YFP vector, which contains a luciferase gene and YFP expression cassette as a control for AAV infection. To confirm the feasibility of these constructs for gene therapy, we examined the ability of AAV-sh-luc-YFP or AAV-sh-Ctsk to infect target cells (osteoclasts) through analysis of the YFP or Ctsk expression. Hence, the WT MBM cells cultured with M-CSF

and RANKL for osteoclastogenesis assays were then transduced with no vector (mock group), AAV-sh-luc-YFP (control group) or AAV-sh-Ctsk to generate pre-osteoclasts and mature osteoclasts. Fluorescence analysis showed that pre-osteoclasts and osteoclasts were efficiently transduced with the AAV-sh-Ctsk or AAV-sh-luc-YFP constructs at a titer of 6×10^{11} DNase-resistant particles/mL (Fig. 1A). Consistently, western blot analysis showed an 80% reduction in Ctsk expression in cells transduced with AAV-sh-Ctsk compared with those transduced with AAV-sh-luc-YFP (Fig. 1B and 1C). Furthermore, cells transduced with AAV-sh-Ctsk had no difference in extracellular acidification compared to cells transduced with AAV-sh-luc-

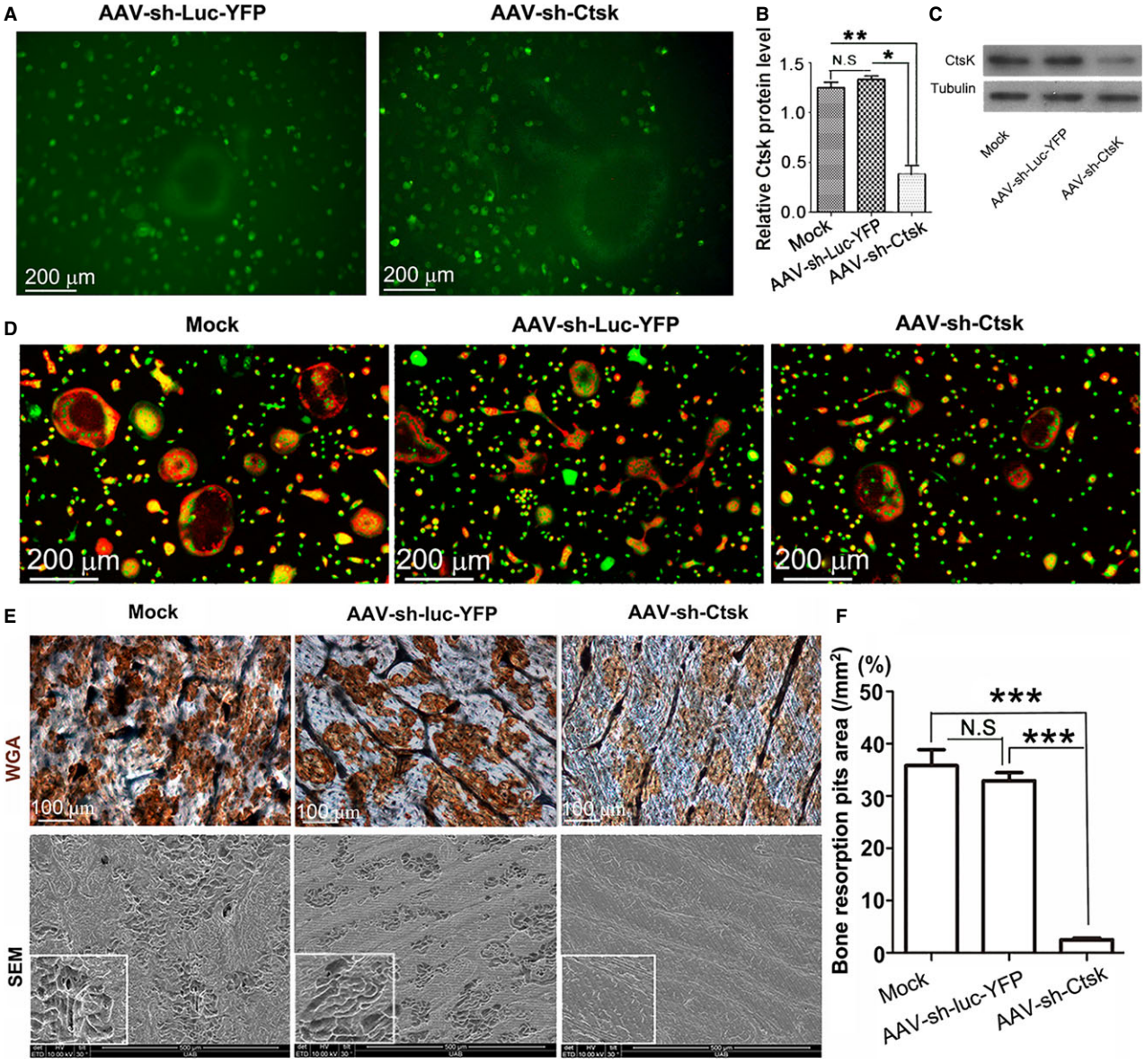

Fig. 1. AAV efficiently transduced osteoclasts and Ctsk knockdown by AAV impairs osteoclast function *in vitro*. (A) Immunofluorescent photomicrograph of AAV-sh-luc-YFP control and AAV-sh-Ctsk treatment groups 7 d after transduction. (B) Western blot analysis of Ctsk expression from the mock-, AAV-sh-luc-YFP– and AAV-sh-Ctsk–treated groups. (C) Quantification of western blot analysis demonstrates that the AAV-sh-Ctsk–treated group showed significant reduction in Ctsk expression as compared to the AAV-sh-luc-YFP control group. (D) Untransduced osteoclasts (mock) and osteoclasts transduced with AAV-sh-Ctsk or AAV-sh-luc-YFP (control) stained with acridine orange to show extracellular acidification. (E) Bone resorption pits were visualized by WGA and SEM analyses. (F) Quantification of bone pits from SEM analysis shows that bone resorption is significantly lower in the AAV-sh-Ctsk–treated group as compared to the mock and AAV-sh-luc-YFP groups ($n = 3$). *$p < 0.05$, **$p < 0.01$, ***$p < 0.001$, NS indicates $p > 0.05$. AAV, adeno-associated virus; Ctsk, cathepsin K; luc, luciferase; SEM, scanning electron microscope; sh, short hairpin; WGA, wheat germ agglutinin; YFP, yellow fluorescent protein.

YFP (control group) or non-infected cells from WT mice (mock control) (Fig. 1D). To establish the effect of AAV-mediated Ctsk knockdown on osteoclast function *in vitro*, bone resorption pits were assessed using WGA, which stains exposed bone matrix proteins, and SEM to visualize bone resorption pits. Data showed that bone resorption by osteoclasts was almost completely blocked by AAV-sh-Ctsk treatment (Fig. 1E, top panel), demonstrating the functional efficiency of AAV-sh-Ctsk as an agent for targeting bone loss (Fig. 1E, bottom panel). Hence, AAV-mediated Ctsk silencing resulted in a significant impairment of bone resorption compared to the control (Fig. 1F). Importantly, these results showed that AAV-sh-Ctsk could effectively inhibit osteoclastic bone resorption *in vitro*. Collectively, these data indicate that AAV-sh-Ctsk can efficiently infect osteoclasts to affect Ctsk expression *in vitro*.

Adeno-associated virus effectively transduces periodontal tissue and displays a local distribution pattern *in vivo*

To evaluate further the potential of AAV-mediated gene therapy as a tool for gene transfer to periodontal tissues, we assessed the ability of AAV-sh-luc-YFP (used as a negative control) to achieve sustained and localized luciferase expression *in vivo*. AAV was administrated into the gingival tissue on the right side of the lower jaw as indicated (Fig. 2A). Data showed that luciferase was not only expressed but also limited to the injection sites after 2 and 5 wk of injection (Fig. 2B). Importantly, luciferase expression was higher after 5 wk of administration as compared to 2 wk, demonstrating that AAV could induce sustained gene expression in gingival tissues. These data show that AAV-mediated gene therapy can effectively transduce periodontal tissues and that injection of AAV into gingival tissue can induce sustained and localized gene expression. Moreover, fluorescent analysis of infected mice treated with AAV-sh-luc-YFP and AAV-sh-Ctsk compared to the uninfected control group further demonstrated that the AAV vectors could successfully infiltrate periodontal tissues (Fig. 2C). Consistent with the *in vitro* data, we showed that whereas TRAP-positive osteoclasts were present around the teeth in the AAV-sh-luc-YFP– or AAV-sh-Ctsk–treated groups, the number of osteoclasts present decreased significantly in the periodontal lesion area in the AAV-sh-Ctsk group (Fig. 2D and 2F). Moreover, IF analysis revealed that Ctsk expression was markedly decreased in the fibroblast and periodontal ligament area of the AAV-sh-Ctsk–treated group compared to the AAV-sh-luc-YFP–treated group (Fig. 2E and 2G), indicating that Ctsk may also have functions in fibroblasts.

Cathepsin K silencing by adeno-associated virus protects mice from periodontitis-induced bone loss

Next, we examined whether Ctsk depletion by local administration of AAV could protect mice from bone loss stemming from *P. gingivalis*-induced periodontitis through analysis of alveolar bone loss in uninfected mice (normal) compared to *P. gingivalis*-infected mice treated with either AAV-sh-Ctsk, AAV-sh-luc-YFP (negative control) or PBS (disease group) (Fig. 3A). Data showed that the AAV-sh-luc-YFP or PBS group had significantly more bone loss compared to the AAV-sh-Ctsk or normal group (Fig. 3B). Moreover, to determine whether the periodontal ligament between the tooth root and the bone was normalized by AAV-sh-Ctsk treatment, we performed hematoxylin and eosin stain analysis on infected mice treated with AAV-sh-Ctsk compared to the AAV-sh-luc-YFP– or PBS-treated group and demonstrated that AAV-sh-Ctsk treatment caused a reduction in *P. gingivalis*-induced periodontal ligament widening and bone loss (Fig. 3C). In addition, the distance between the tooth root surface and the alveolar bone was decreased in half in the AAV-sh-Ctsk and disease group as compared to the AAV-sh-luc-YFP group (Fig. 3C and 3D), demonstrating that AAV-sh-Ctsk can prevent periodontal ligament damage.

Cathepsin K silencing by adeno-associated virus reduces T cells and dendritic cells in alveolar bone

To examine the effects of AAV-mediated Ctsk silencing on T cells *in vivo*, tooth root sections were subjected to IF staining using to analyze CD3-positive T cells (Fig. 3E). Data revealed that T cells in the periodontal ligament were significantly decreased in the AAV-sh-Ctsk treatment group as compared to the AAV-sh-luc-YFP and PBS groups (Fig. 3E and 3F). In addition, we performed IF staining for analysis of dendritic cells (DCs) in uninfected mice (normal) and *P. gingivalis*-infected mice treated with AAV-sh-Ctsk, PBS or AAV-sh-luc-YFP by co-expression of Ctsk and CD11c. Data showed that the number of CD11c-positive DCs in the AAV-sh-Ctsk–treated group was decreased significantly, indicating an increase in DCs in the periodontal lesion area of the AAV-sh-luc-YFP control group and PBS disease control group (Fig. 4). Notably, our data also revealed that Ctsk was expressed in DCs, suggesting that Ctsk may also carry important functions in immune response cells. Collectively, the results indicate that Ctsk depletion by AAV not only protects mice from *P. gingivalis*-induced bone loss, but also reduces immune response *in vivo* and protects against inflammation caused by periodontal disease.

Cathepsin K silencing by adeno-associated virus attenuates the expression of osteoclast marker genes and cytokines in periodontal lesions

To determine further the impact of AAV-mediated Ctsk depletion on the inflammatory response, qRT-PCR was used to examine the expression level of the inflammatory markers *IL-1*α and *IL-1*β in the periodontal tissues of the different experiment groups. *IL-1*α and *IL-1*β *expression* was higher in the AAV-sh-luc-YFP

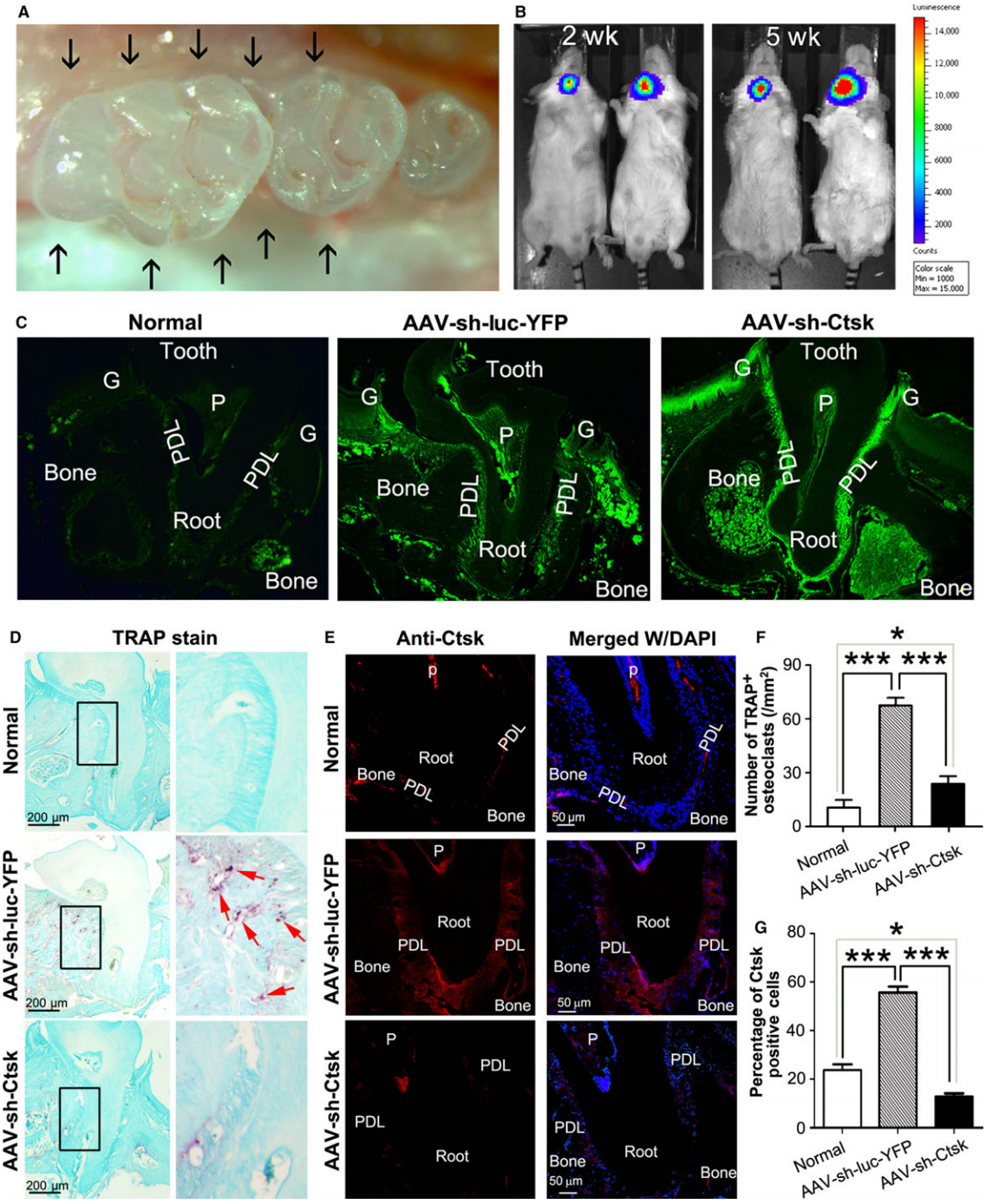

Fig. 2. AAV can effectively transduce periodontal tissue, display a local distribution pattern and inhibit osteoclast differentiation *in vivo*. (A) Mouse maxillary molars showing the sites of AAV administration (black arrows). (B) Analysis at 2 and 5 wk after a single administration of AAV-sh-luc-YFP into the lower right jaw. Luciferase expression was sustained and limited to the local injection sites ($N = 15$, $n = 5$ samples in each group; experiments were repeated three times). (C) Fluorescent micrographs of AAV-infected cells in uninfected mice and infected mice treated with AAV-sh-Ctsk and AAV-sh-luc-YFP ($N = 15$, $n = 5$ samples in each group; experiments were repeated three times). (D) TRAP staining reveals the presence of osteoclasts surrounding the tooth root structures in both AAV-sh-luc-YFP– and AAV-sh-Ctsk–treated groups ($n = 3$). (E) Localization of Ctsk expression (red, anti-Ctsk; blue, nuclei counterstaining with Hoechst 33342) in the murine periodontal tissue transduced with AAV-sh-luc-YFP or AAV-sh-Ctsk ($n = 3$). (F) Quantification of TRAP-positive osteoclasts in lesion areas. (G) Quantification of Ctsk-positive cells in periodontal tissue area. $*p < 0.05$, $***p < 0.001$, NS indicates $p > 0.05$. AAV, adeno-associated virus; Ctsk, cathepsin K; G, gingival; luc, luciferase; P, pulp; PDL, periodontal ligament; SEM, scanning electron microscope; sh, short hairpin; TRAP, tartrate-resistant acid phosphatase; W/, with; WGA, wheat germ agglutinin; YFP, yellow fluorescent protein.

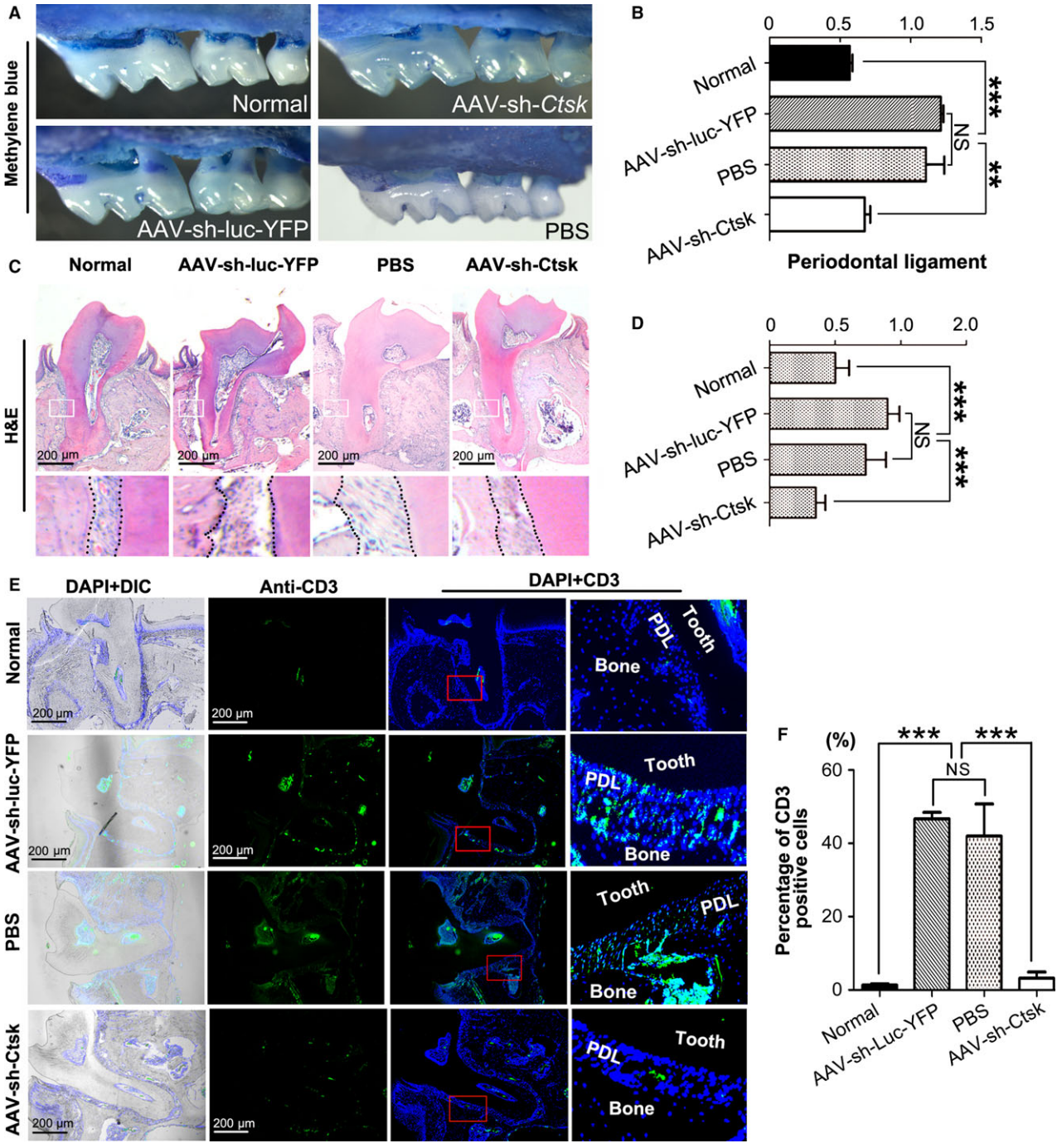

Fig. 3. Ctsk silencing by AAV protects mice from bone loss in *P. gingivalis*-induced periodontitis. (A) Periodontitis as indicated by alveolar bone loss and root exposure was examined in normal group vs. *P. gingivalis*-infected mice treated with AAV-sh-Ctsk, AAV-sh-luc-YFP or PBS. (B) Quantification of bone resorption in the normal group, AAV-sh-luc-YFP–, PBS- and AAV-sh-Ctsk–treated groups ($N = 21$, $n = 7$, repeated three times). (C) Hematoxylin and eosin staining of sections from uninfected mice (normal) and *P. gingivalis*-infected mice treated with AAV-sh-Ctsk, AAV-sh-luc-YFP or PBS. (D) The width of periodontal ligament in the uninfected mice and *P. gingivalis*-infected mice treated with AAV-sh-Ctsk, AAV-sh-luc-YFP or PBS ($N = 15$, $n = 5$, repeated three times). (E) Immunofluorescent colony staining of alveolar sections from different groups. Cell nuclei were labeled using DAPI staining (blue). Blue and green fluorescence merged with bright DIC and DAPI shows the shape of the tooth ($N = 15$, $n = 5$, repeated three times). (F) Quantification of CD3-positive T cells shows a significant reduction in T-cell number in the AAV-sh-Ctsk group as compared to the AAV-sh-luc-YFP and PBS group. $^{**}p < 0.01$, $^{***}p < 0.001$, NS indicates $p > 0.05$. AAV, adeno-associated virus; Ctsk, cathepsin K; DIC, differential interference contrast; H&E, hematoxylin and eosin; luc, luciferase; PBS, phosphate-buffered saline; sh, short hairpin; PDL, periodontal ligament; YFP, yellow fluorescent protein.

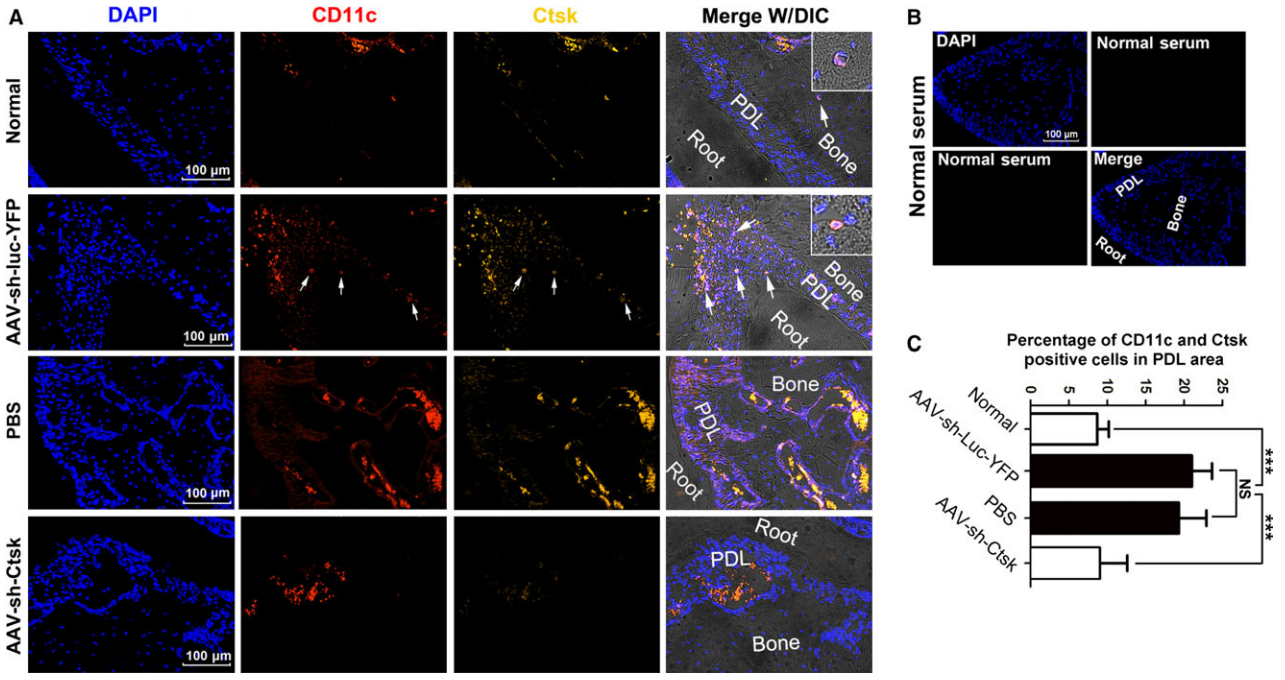

Fig. 4. Ctsk knockdown decreases the number of CD11c and Ctsk double-positive cells in periodontal lesion areas. (A) Immunofluorescent colony staining of CD11c (red) and Ctsk (yellow) double-positive DCs in the periodontal lesion area in uninfected mice (normal) and *P. gingivalis*-infected mice treated with AAV-sh-Ctsk, AAV-sh-luc-YFP and PBS ($N = 15$, $n = 5$, repeated three times) at 56 d. Blue and green fluorescence merged with bright DIC and DAPI shows the shape of the periodontal tissue. (B) Normal serum served as a negative control of the same area (without primary antibody). (C) Quantification of double-positive DCs analysis demonstrates that Ctsk has significantly reduced expression of CD11c (red) and Ctsk (yellow) double-positive DCs in different groups. ***$p < 0.001$. AAV, adeno-associated virus; Ctsk, cathepsin K; DCs, dendritic cells; DIC, differential interference contrast; luc, luciferase; NS, no significance; PBS, phosphate-buffered saline; PDL, periodontal ligament; sh, short hairpin; W/, with; YFP, yellow fluorescent protein.

group as compared to the AAV-sh-Ctsk–treated group (Fig. 5A). Furthermore, when compared to the normal group, *IL*-6 expression was increased in *P. gingivalis*-infected mice treated with the control AAV-sh-luc-YFP group. Further analysis showed that the expression of *acid phosphatase 5, tartrate resistant (Acp5)*, an osteoclast marker gene, was comparable in either the AAV-sh-luc-YFP group or the AAV-sh-Ctsk–treated group (Fig. 5A). We noted that whereas the expression of osteoprotegrin (*OPG*), an inhibitor of osteoclastogenesis, was decreased in the AAV-sh-luc-YFP–treated group, RANKL displayed an inversed expression pattern in these groups (Fig. 5A). The finding was further confirmed by analysis of IL-1α by ELISA (Fig. 5B). The expression levels of the proinflammatory cytokines IL-17, TNFα, IL-12 and interferon-gamma were also higher in the AAV-sh-luc-YFP group as compared to the AAV-sh-Ctsk control and uninfected groups (Fig. 5B). The anti-inflammatory cytokine IL-10 was increased in the AAV-sh-Ctsk–treated group but not in the AAV-sh-luc-YFP–treated group (Fig. 5B), suggesting an inhibition in the inflammation response in the AAV-sh-Ctsk–treated group. These results indicate that Ctsk knockdown reduces expression of genes important for osteoclastic bone resorption and inflammation in periodontal tissues.

Discussion

Local administration of adeno-associated virus-short hairpin-cathepsin K gene therapy is a promising therapeutic strategy for periodontal disease

Current therapies for periodontal disease are focused on antimicrobial treatments and surgery, which bear limited efficacy (21). AAV-mediated gene therapy carries great potential for treating periodontitis through maintenance of sustainable endogenous gene in a non-invasive manner (22,23). However, it remains to be determined which genes and AAV vectors that can be safely used to induce effective gene expression in local periodontal tissues. This is a fundamental issue that needs to be addressed to develop potent and safe AAV-mediated gene therapy for periodontal disease (23). Notably, intra-articular administration of AAV2 has been shown to trigger sustainable gene expression for 120 d (24). Hence, we utilized the AAV2 serotype to subclone a shRNA construct, which targets Ctsk into the AAV.H1 vector, which was successfully used *in vivo* to knockdown estrogen receptor-α expression in the brain (12). In line with this finding, we demonstrated that AAV could also effectively infect periodontal tissues to transfer a specific gene. After one local injection of AAV-sh-luc-YFP, which contains

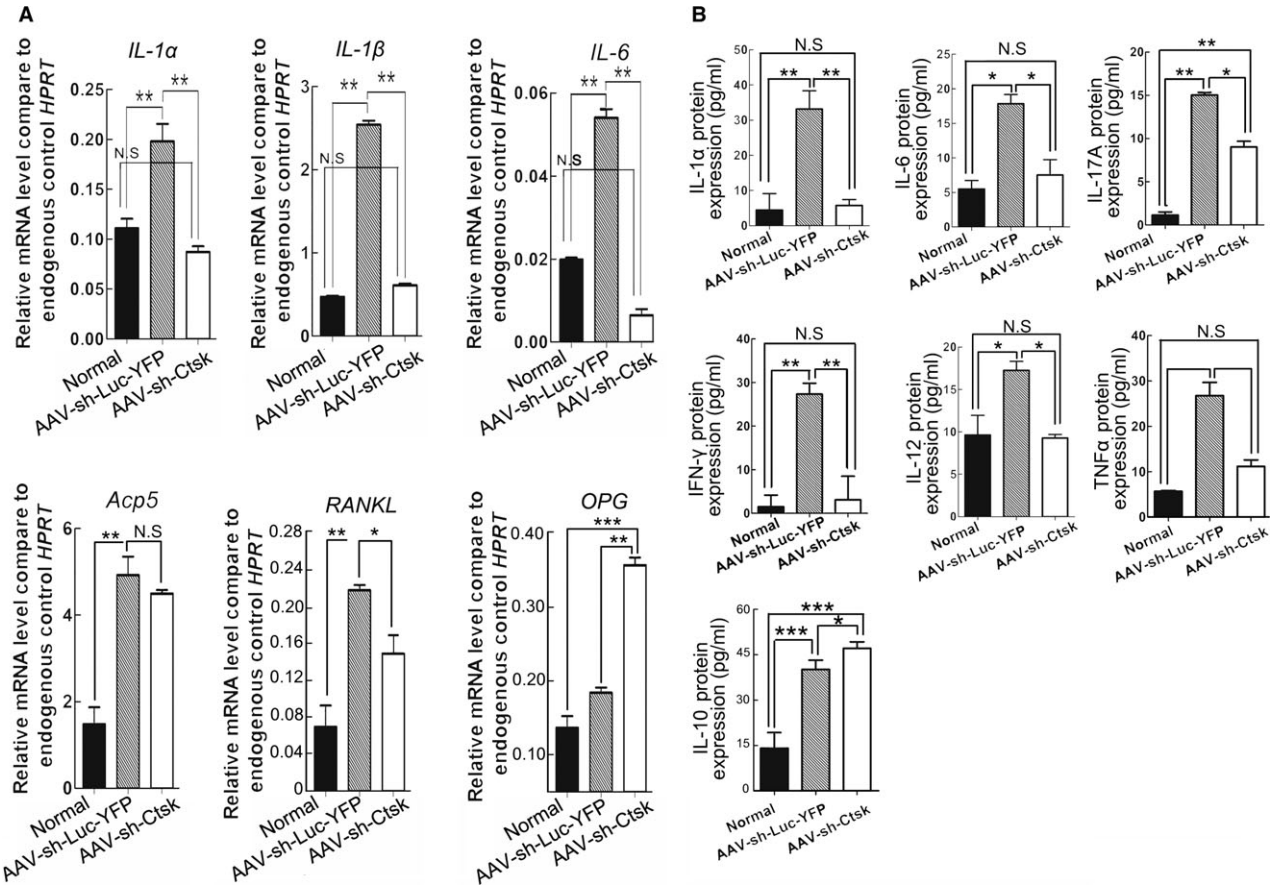

Fig. 5. AAV-sh-Ctsk reduces the expression of inflammatory factors in the periodontal tissues. (A) Quantitative reverse transcription–polymerase chain reaction of osteoclast-specific genes (i.e. Acp5, RANKL and OPG) and inflammatory cytokines (IL-1α, IL-1β and IL-6) in the periodontal tissues of uninfected mice (normal) or *P. gingivalis*-infected mice treated with AAV-sh-luc-YFP or with AAV-sh-Ctsk. Expression levels were normalized to Hprt ($N = 15$, $n = 5$, repeated three times). (B) Level of inflammatory factors IL-1α, IL-6, IL-12, IL-17A, TNF-α, IFN-γ and IL-10 in the periodontal tissues as detected by enzyme-linked immunosorbent assay (pooled three samples each time in each group on three independent experiments). $^{*}p < 0.05$, $^{**}p < 0.01$, $^{***}p < 0.001$, NS indicates $p > 0.05$. AAV, adeno-associated virus; Ctsk, cathepsin K; Hprt, hypoxanthine–guanine phosphoribosyl transferase; IL, interleukin; IFN, interferon; luc, luciferase; NS, not significant; OPG, osteoprotegrin; RANKL, receptor activator of the NF-κβ ligand; sh, short hairpin; TNF, tumor necrosis factor; YFP, yellow fluorescent protein.

YFP and luciferase genes, luciferase expression was sustained and limited to the local injection sites for at least 5 wk. A sustainable YFP expression was observed in gingival tissue, periodontal ligament and dental pulp tissue. Most importantly, luciferase expression was limited to the local administrated areas. It is well documented that AAV vectors do not contain viral genes that could elicit undesirable cellular immune responses and generally appear not to induce inflammatory responses (25). Consistent with the essential role of Ctsk in osteoclast function, local administration of AAV-sh-Ctsk gene therapy carries great potential for effectively and safely targeting bone loss that results from oral infectious diseases such as periodontitis.

Adeno-associated virus-short hairpin-cathepsin K knockdown can inhibit cathepsin K expression and bone resorption *in vitro* and *in vivo*

Our investigation of the effects of AAV-mediated Ctsk knockdown on osteoclast function *in vitro* was carried out through analysis of bone resorption using WGA and SEM. Our results revealed that AAV-mediated Ctsk depletion caused a drastic impairment in bone resorption *in vitro* ($p < 0.001$). Consistent with that posture, TRAP staining showed a significant decrease in TRAP-positive osteoclasts *in vivo* in the AAV-sh-Ctsk–treated group as compared to the AAV-sh-luc-YFP group. Periodontal ligament cells are fibroblast-like cells characterized by collagen production as well as cytokine and chemokine release, which can contribute to periodontal inflammation (26). Notably, we found that Ctsk was highly expressed in the periodontal ligament area in the AAV-sh-luc-YFP group by IF staining, which suggest an important role for Ctsk in fibroblast-like cells. Osteoclasts are the only well studied cell type that can mediate the bone resorption

(27,28). Notably, recent studies have indicated that osteoclast activation is not only solely dependent on osteoblasts, but it may also be dependent on other cells present in the local bone environment. Given that DCs, macrophages and osteoclasts are all originated from the hematopoietic cell lineage, it is believed that osteoclasts are closely related to the immune cells, which may affect osteoclast formation and/or function through formation of different types of terminal cells in their local environment (29–31). It was recently reported that whereas the Ctsk knockout in mouse displayed normal osteoclast numbers but non-functional osteoclasts as assessed by their inabilities to resorb bone matrix, indicating that Ctsk is critical for osteoclast function but may play a dispensable role in osteoclast differentiation (32). Unlike the finding from Ctsk knockout mice, our data showed that osteoclast numbers were decreased in the AAV-sh-Ctsk–treated group, suggesting that the knockdown of Ctsk may affect osteoclast activation through its effect on immune cells. Further studies are needed to assess the role of Ctsk in osteoclastogenesis in the context of the bone microenvironment under inflammatory stimulation.

Adeno-associated virus-mediated cathepsin K by adeno-associated virus can effectively target both inflammation and bone loss in periodontitis

Bone resorption and inflammation are two key challenges in oral health because oral bacteria can strongly stimulate T- and B-cell activation. The latter can strongly promote osteoclast formation and function, which can ultimately lead to bone loss around the teeth (33,34). We previously characterized the role of Ctsk in osteoclasts and revealed that Ctsk is crucial for osteoclastic bone resorption (19,35). It was recently reported that Ctsk inhibition could suppress autoimmune inflammation of the joints as well as bone resorption in autoimmune arthritis and that *Ctsk*$^{-/-}$ rats were resistant to experimental autoimmune encephalomyelitis (36). Collectively, these findings suggest that Ctsk plays an important role in the immune system aside from its role in osteoclasts and may thus serve as an important therapeutic target for targeting autoimmune diseases (36–38). Notably, these dual roles of Ctsk in osteoclast and immune functions make it an ideal candidate for targeting both inflammation and bone loss resorption in many inflammatory bone diseases. Indeed, local administration of AAV-sh-Ctsk can not only reduce bone loss and inflammation in periodontitis, as in our current study, but it can also inhibit periapical bone loss and inflammation in a mouse model of endodontic disease as we previously reported (39). Therefore, AAV-sh-Ctsk may be useful for targeting the interplays of osteoclastic bone resorption and activated immune functions in many inflammatory diseases. In this current study, we investigated the dual functions of Ctsk in relationship to periodontal disease. We revealed that treatment of periodontitis induced in mice by *P. gingivalis* infection with AAV-sh-Ctsk could protect mice from *P. gingivalis*-stimulated alveolar bone loss. Notably, AAV-sh-Ctsk treatment can also attenuate inflammation in *P. gingivalis*-induced periodontitis by, in part, decreasing T cells and DC numbers in the periodontal lesions. In our current experiment, the PBS and AAV-sh-luc-YFP were chosen as the disease control group, which the YFP group is a better control group for the AAV-sh-Ctsk group as the YFP group also contains the AAV. This can show that the AAV itself does not have any bone protection effect compared to the target gene. The PBS group was applied to show that the periodontitis mouse model is successful and stable.

The underlying mechanism of cathepsin K functions is different in periodontitis from periapical disease

Furthermore, we explored the functions of the Ctsk using, in this established mouse periodontitis model induced by infection with *P. gingivalis* W50, a known pathogen that is highly associated with periodontal disease progression by stimulating both inflammation and bone resorption, two key features of periodontitis (40). In addition, the host immune and inflammatory response play important roles in periodontitis (1,2). In our previous study, we applied four different bacterial strains to generate a periapical disease model to investigate the role of Ctsk in this disease (39). Whereas inflammation associated with periapical disease is mainly localized to the oral cavity, inflammation in periodontitis stems mostly from systemic reactions, which can trigger other diseases (41). These findings indicate that the molecular mechanism by which the Ctsk functions in the periodontitis model is different from its role in periapical disease. We demonstrated that AAV-mediated Ctsk in periodontitis inhibits bone resorption and attenuates local inflammation. Specifically, AAV-sh-Ctsk caused downregulation of many inflammatory cytokines in the periodontal tissues was assessed by ELISA and qRT-PCR analyses. The reduction in inflammation in the AAV-sh-Ctsk treatment group may also be partially due to downregulation of IL-6, which can promote the activation and differentiation of the macrophages. In fact, IL-6 can be secreted by osteoblasts in response to bone resorbing agents such as IL-1α, IL-1β and TNFα (42). Ctsk has been reported to have functions in DCs through toll-like receptors (TLRs) (36). Our results through co-expression of CD11c and Ctsk support that Ctsk may simultaneously stimulate functions of the DCs and osteoclast function. Hence, our finding that expression of IL-6, IL-12 and TNFα was attenuated by the AAV-mediated Ctsk depletion may stem from the inhibition of Ctsk functions in DCs, which should further be validated by *in vitro* study. In further understanding the molecular mechanisms underlying the protection from periodontitis-induced bone loss with Ctsk deletion, we revealed that while expression of the osteoclast marker *Acp5* in the periodontitis lesion area was almost unaffected by AAV-mediated Ctsk

knockdown, there was a block in bone turnover in the periodontitis, which was due to an increase in OPG and a decrease in RANKL expression. This finding is inconsistent with other reports demonstrating that RANKL is also expressed in inflammatory cells (mainly lymphocytes and macrophages) and proliferating epithelium near inflammatory cells (43). Hence, the decrease in RANKL expression may be the result of attenuated inflammation by depletion of the Ctsk in periodontitis lesions. Owing to the limited tissue available for ELISA assays, we chose to examine the expression level of known inflammatory factors, including IL-1α, IL-1β, TNFα, IL-6, IL-12 and IL-10, which can provide great mechanistic information on the functions of the Ctsk in periodontitis. Furthermore, such analysis can help explain whether these expression changes can promote innate immune responses from tissue epithelia to limit the damage caused by viral and bacterial infections. These cytokines can also facilitate the tissue-healing process in injuries caused by infection or inflammation. TNFα and IL-1α have been indicated as potent stimulators of bone resorption, and they have been found in the periodontitis lesion area (44,45). IL-1β is another inflammation factor that is connected with gingival inflammation (46). IL-6 may have a proinflammatory function by increasing its levels and reabsorbing bone in the presence of inflammatory factors such as TNFα and IL-1α (47). IL-12 can stimulate interferon-gamma production through T-helper type 1 cells, which are considered to have a connection with the severity of periodontitis (48). All of these markers were downregulated after the Ctsk was knocked down, which indicated that the Ctsk deficiency might impair the immune response in the periodontitis local lesion area. It has been reported that Ctsk is expressed in DCs (36). Notably, our immunofluorescence data showed that the number of DCs decreased significantly in the lesion area. Notably, IL-10 can also repress proinflammatory responses and limit tissue damage caused by inflammation, which support crucial roles for the IL-10 family of cytokines in many infectious and inflammatory diseases (49). Collectively, our data demonstrate that AAV-mediated Ctsk silencing therapy can provide the unique opportunity to address the interconnected issues of inflammation and bone resorption in periodontitis.

Although, it is difficult to define the exact details of the mechanism at this point, we can determine that Ctsk knockdown results in defective TLR9 signaling in DCs in response to bacterial infection as shown by the reduced mRNA level of proinflammatory cytokines (e.g. IL-12 and IL-6) that are regulated by TLR9 (Fig. 5). This finding is consistent with that reported by Asagiri *et al.* (36) in a study using a mouse model of experimental arthritis in which the Ctsk inhibitor reduced the TLR9-mediated immune response as shown by a reduction in cytokine (e.g. IL-12 and IL-6) mRNA. We further determined that the Ctsk knockdown in periodontal lesions results in defective TLR4 signaling because the expression of TNFα was reduced in the lesion area. Our data indicate a dramatic reduction in Ctsk expression after Ctsk knockdown *in vitro* (Fig. 1F) and *in vivo* (Fig. 2F). Importantly, the AAV-sh-Ctsk is administered after the immune response, inflammation and bone resorption have already been initiated, as would be the case in the clinic. Notably, the Asagiri *et al.* (36) study did not examine bone resorption like our study.

In summary, our local administration of the sh-Ctsk through AVV-mediated gene therapy can inhibit, simultaneously and effectively both inflammation and osteoclastic bone resorption in *P. gingivalis*-induced periodontitis after these processes have already been initiated, as would be the case in the clinic. Importantly, AAV gene therapy has been used in numerous studies to target many human diseases and thus carry great therapeutic potential for periodontal disease. Given the dual roles of the Ctsk in promoting inflammation and osteoclastic bone resorption, utilization of this promising AAV technology to target the Ctsk offers a unique tool to simultaneously target bone resorption and inflammation with limited side effects in numerous diseases, including oral infectious diseases, rheumatoid arthritis and bone metastases.

Acknowledgements

We thank Ms. Christie Paulson for her excellent assistance with this manuscript. We appreciate the assistance of the Center for Metabolic Bone Disease at The University of Alabama at Birmingham (P30 AR046031). We are also grateful for the assistance of the Small Animal Phenotyping Core (P30 DK079626), Metabolism Core, and Neuroscience Molecular Detection Core Laboratory at the University of Alabama at Birmingham (P30 NS0474666). This work was supported by R01DE023813 (Y.P.L.) and UAB Department of Pathology Start-Up funding (Wei Chen).

Conflicts of interest

The authors declare no potential conflicts of interest with respect to the authorship and/or publication of this article.

Supporting Information

Additional Supporting Information may be found in the online version of this article:

Data S1 Materials and methods.

Figure S1 Timeline for bacterial infection and AAV treatment.

Table S1 Description of the AAV-shRNA-Ctsk treatment group and experimental control groups using BALB/cJ mice with and without *P. gingivalis* W50 infection.

Table S2 qRT-PCR Taqman probe numbers.

References

1. Sasaki H, Okamatsu Y, Kawai T, Kent R, Taubman M, Stashenko P. The interleukin-10 knockout mouse is highly susceptible to Porphyromonas gingivalis-induced alveolar bone loss. *J Periodontal Res* 2004;**39**:432–441.
2. Wilensky A, Polak D, Awawdi S, Halabi A, Shapira L, Houri-Haddad Y. Strain-dependent activation of the mouse

immune response is correlated with *Porphyromonas gingivalis*-induced experimental periodontitis. *J Clin Periodontol* 2009;**36**:915–921.
3. Seckin Ertugrul A, Arslan U, Dursun R, Sezgin Hakki S. Periodontopathogen profile of healthy and oral lichen planus patients with gingivitis or periodontitis. *Int J Oral Sci* 2013;**5**:92–97.
4. Darveau RP. Periodontitis: a polymicrobial disruption of host homeostasis. *Nat Rev Microbiol* 2010;**8**:481–490.
5. Fischer CL, Walters KS, Drake DR *et al*. Oral mucosal lipids are antibacterial against *Porphyromonas gingivalis*, induce ultrastructural damage, and alter bacterial lipid and protein compositions. *Int J Oral Sci* 2013;**5**:130–140.
6. Li YP, Alexander M, Wucherpfennig AL, Yelick P, Chen W, Stashenko P. Cloning and complete coding sequence of a novel human cathepsin expressed in giant cells of osteoclastomas. *J Bone Miner Res* 1995;**10**:1197–1202.
7. Gelb BD, Shi GP, Chapman HA, Desnick RJ. Pycnodysostosis, a lysosomal disease caused by cathepsin K deficiency. *Science* 1996;**273**:1236–1238.
8. Bankiewicz KS, Forsayeth J, Eberling JL *et al*. Long-term clinical improvement in MPTP-lesioned primates after gene therapy with AAV-hAADC. *Mol Ther* 2006;**14**:564–570.
9. Wang L, Cao O, Swalm B, Dobrzynski E, Mingozzi F, Herzog RW. Major role of local immune responses in antibody formation to factor IX in AAV gene transfer. *Gene Ther* 2005;**12**:1453–1464.
10. Kaplitt MG, Feigin A, Tang C *et al*. Safety and tolerability of gene therapy with an adeno-associated virus (AAV) borne GAD gene for Parkinson's disease: an open label, phase I trial. *Lancet* 2007;**369**:2097–2105.
11. Feng SM, Deng LF, Chen W, Shao JZ, Xu GL, Li YP. Atp6v1c1 is an essential component of the osteoclast proton pump and in F-actin ring formation in osteoclasts. *Biochem J* 2009;**417**:195–203.
12. Musatov S, Chen W, Pfaff DW, Kaplitt MG, Ogawa S. RNAi-mediated silencing of estrogen receptor alpha in the ventromedial nucleus of hypothalamus abolishes female sexual behaviors. *Proc Natl Acad Sci USA* 2006;**103**:10456–10460.
13. Hommel JD, Sears RM, Georgescu D, Simmons DL, DiLeone RJ. Local gene knockdown in the brain using viral-mediated RNA interference. *Nat Med* 2003;**9**:1539–1544.
14. Tu Q, Zhang J, Fix A *et al*. Targeted overexpression of BSP in osteoclasts promotes bone metastasis of breast cancer cells. *J Cell Physiol* 2009;**218**:135–145.
15. Jiang H, Chen W, Zhu G *et al*. RNAi-mediated silencing of Atp6i and Atp6i haploinsufficiency prevents both bone loss and inflammation in a mouse model of periodontal disease. *PLoS ONE* 2013;**8**:e58599.
16. Yang S, Hao L, McConnell M *et al*. Inhibition of Rgs10 expression prevents immune cell infiltration in bacteria-induced inflammatory lesions and osteoclast-mediated bone destruction. *Bone Res* 2013;**1**:267–281.
17. Yang SY, Li YP. RGS10-null mutation impairs osteoclast differentiation resulting from the loss of $[Ca^{2+}]_i$ oscillation regulation. *Genes Dev* 2007;**21**:1803–1816.
18. Yang S, Wei D, Wang D, Phimphilai M, Krebsbach PH, Franceschi RT. In vitro and in vivo synergistic interactions between the Runx2/Cbfa1 transcription factor and bone morphogenetic protein-2 in stimulating osteoblast differentiation. *J Bone Miner Res* 2003;**18**:705–715.
19. Chen W, Yang SY, Abe Y *et al*. Novel pycnodysostosis mouse model uncovers cathepsin K function as a potential regulator of osteoclast apoptosis and senescence. *Hum Mol Genet* 2007;**16**:410–423.
20. Chen W, Ma J, Zhu G *et al*. Cbfβ deletion in mice recapitulates cleidocranial dysplasia and reveals multiple functions of Cbfβ required for skeletal development. *Proc Natl Acad Sci USA* 2014;**111**:8482–8487.
21. Goodson JM, Haffajee AD, Socransky SS *et al*. Control of periodontal infections: a randomized controlled trial I. The primary outcome attachment gain and pocket depth reduction at treated sites. *J Clin Periodontol* 2012;**39**:526–536.
22. Evans C. Arthritis gene therapy trials reach phase II. *J Rheumatol* 2010;**37**:683–685.
23. Mease PJ, Wei N, Fudman EJ *et al*. Safety, tolerability, and clinical outcomes after intraarticular injection of a recombinant adeno-associated vector containing a tumor necrosis factor antagonist gene: results of a phase 1/2 study. *J Rheumatol* 2010;**37**:692–703.
24. Zhou Q, Guo RL, Wood R *et al*. Vascular endothelial growth factor c attenuates joint damage in chronic inflammatory arthritis by accelerating local lymphatic drainage in mice. *Arthritis Rheum* 2011;**63**:2318–2328.
25. Carter BJ. Adeno-associated virus vectors in clinical trials. *Hum Gene Ther* 2005;**16**:541–550.
26. Jönsson D, Nebel D, Bratthall G, Nilsson BO. The human periodontal ligament cell: a fibroblast-like cell acting as an immune cell. *J Periodontal Res* 2011;**46**:153–157.
27. Chen W, Zhu G, Hao L, Wu M, Ci H, Li Y-P. C/EBPα regulates osteoclast lineage commitment. *Proc Natl Acad Sci* 2013;**110**:7294–7299.
28. Li YP, Chen W, Liang Y, Li E, Stashenko P. Atp6i-deficient mice exhibit severe osteopetrosis due to loss of osteoclast-mediated extracellular acidification. *Nat Genet* 1999;**23**:447–451.
29. O'Gradaigh D, Compston JE. T-cell involvement in osteoclast biology: implications for rheumatoid bone erosion. *Rheumatology* 2004;**43**:122–130.
30. Takayanagi H. Osteoimmunology: shared mechanisms and crosstalk between the immune and bone systems. *Nat Rev Immunol* 2007;**7**:292–304.
31. Nakashima T, Takayanagi H. Osteoclasts and the immune system. *J Bone Miner Metab* 2009;**27**:519–529.
32. Saftig P, Hunziker E, Wehmeyer O *et al*. Impaired osteoclastic bone resorption leads to osteopetrosis in cathepsin-K-deficient mice. *Proc Natl Acad Sci USA* 1998;**95**:13453–13458.
33. Lappin DF, Macleod CP, Kerr A, Mitchell T, Kinane DF. Anti-inflammatory cytokine IL-10 and T cell cytokine profile in periodontitis granulation tissue. *Clin Exp Immunol* 2001;**123**:294–300.
34. Manhart SS, Reinhardt RA, Payne JB *et al*. Gingival cell IL-2 and IL-4 in early-onset periodontitis. *J Periodontol* 1994;**65**:807–813.
35. Li Y-P, Chen W. Characterization of mouse cathepsin K gene, the gene promoter, and the gene expression. *J Bone Miner Res* 1999;**14**:487–499.
36. Asagiri M, Hirai T, Kunigami T *et al*. Cathepsin K-dependent toll-like receptor 9 signaling revealed in experimental arthritis. *Science* 2008;**319**:624–627.
37. Kamolmatyakul S, Chen W, Li YP. Interferon-gamma down-regulates gene expression of cathepsin K in osteoclasts and inhibits osteoclast formation. *J Dent Res* 2001;**80**:351–355.
38. Kamolmatyakul S, Chen W, Yang S *et al*. IL-1alpha stimulates cathepsin K expression in osteoclasts via the tyrosine kinase-NF-kappaB pathway. *J Dent Res* 2004;**83**:791–796.
39. Gao B, Chen W, Hao L *et al*. Inhibiting periapical lesions through AAV-RNAi silencing of cathepsin K. *J Dent Res* 2013;**92**:180–186.
40. Haffajee AD, Socransky SS. Microbial etiological agents of destructive periodontal diseases. *Periodontol 2000* 1994;**5**:78–111.
41. Seymour GJ, Ford PJ, Cullinan MP, Leishman S, Yamazaki K. Relationship between periodontal infections and systemic disease. *Clin Microbiol Infect* 2007;**13**(Suppl 4):3–10.
42. Irwin CR, Myrillas TT. The role of IL-6 in the pathogenesis of periodontal disease. *Oral Dis* 1998;**4**:43–47.
43. Liu D, Xu JK, Figliomeni L *et al*. Expression of RANKL and OPG mRNA

in periodontal disease: possible involvement in bone destruction. *Int J Mol Med* 2003;**11**:17–21.
44. Shirodaria S, Smith J, McKay IJ, Kennett CN, Hughes FJ. Polymorphisms in the IL-1A gene are correlated with levels of interleukin-1α protein in gingival crevicular fluid of teeth with severe periodontal disease. *J Dent Res* 2000;**79**:1864–1869.
45. Delima AJ, Oates T, Assuma R *et al*. Soluble antagonists to interleukin-1 (IL-1) and tumor necrosis factor (TNF) inhibits loss of tissue attachment in experimental periodontitis. *J Clin Periodontol* 2001;**28**:233–240.
46. Miller CS, King CP Jr, Langub MC, Kryscio RJ, Thomas MV. Salivary biomarkers of existing periodontal disease: a cross-sectional study. *J Am Dent Assoc* 2006;**137**:322–329.
47. Azuma MM, Samuel RO, Gomes-Filho JE, Dezan-Junior E, Cintra LTA. The role of IL-6 on apical periodontitis: a systematic review. *Int Endod J* 2014;**47**:615–621.
48. Orozco A, Gemmell E, Bickel M, Seymour GJ. Interleukin-1beta, interleukin-12 and interleukin-18 levels in gingival fluid and serum of patients with gingivitis and periodontitis. *Oral Microbiol Immunol* 2006;**21**:256–260.
49. Ouyang W, Rutz S, Crellin NK, Valdez PA, Hymowitz SG. Regulation and functions of the IL-10 family of cytokines in inflammation and disease. *Annu Rev Immunol* 2011;**29**:71–109.